JMEPEG (2004) 13:588-592
DOI: 10.1361/10599490420656

1059-9495/$19.00

Mechanical Properties of Borosilicate Glass Coated With Pure Aluminum by Sputtering

Toshihiko Hoshide and Maki Akamatsu

(*Submitted January 16, 2004*)

Borosilicate glass was coated with pure aluminum by the radio frequency (RF) magnetron-sputtering method under various conditions. The mechanical properties of coated materials were investigated with respect to the sputtering conditions. The surface roughness (R_a) and porosity (p) measured on the coating increased when the initial temperature of the substrate (T_{si}) was increased. A positive correlation between R_a and p also was confirmed. The hardness of aluminum-coated material was measured by using a Vickers microhardness tester. The hardness was greater in materials processed at higher T_{si}, although the hardness hardly depended on the RF output power, P_{RF}. However, the hardness of materials coated under every condition was inferior to that of the substrate glass. Strength tests of coated materials and the substrate glass also were conducted under three-point bending mode. The bending strength (σ_{fm}) of the coated material decreased with increasing T_{si}, although it was better than that of the substrate glass. A good correlation between σ_{fm} and hardness was observed for coated materials, irrespective of the sputtering condition.

Keywords aluminum, bending strength, borosilicate glass, coated materials, hardness, porosity, sputtering

1. Introduction

Glass materials coated with ceramic or metallic films by sputtering are being developed for various engineering applications. As reported in recent works, glass sputtered with a ceramic or metallic thin film is expected to be used for magnetic/electronic devices[1-3] as well as for optical devices.[1,4-7] When coated glass materials are applied functionally as well as mechanically, there is the possibility that they may suffer serious damage due to unexpected forces during anomalous operation or through inconsistency in equipment. Consequently, the mechanical properties of coated glass materials should be clarified to improve their durability in practical applications.

In the present work, the mechanical properties of a borosilicate glass coated with pure aluminum (Al) were investigated experimentally. The present material system, aluminum-silicate, was selected as a model material of interconnect (IC) wiring. Radio frequency (RF) magnetron sputtering was used to produce the thin films on the borosilicate glass. Coated glass samples were prepared under various sputtering conditions by changing the RF output power and substrate temperature. The hardness of the coated glass is an important factor for tribological usage,[8] and the information on material strength is also required for determining the integrity of the bilayer system. The hardness tests were carried out for coated materials and the substrate glass. Since tensile tests of brittle glass or ceramic materials are very difficult to perform to evaluate their strength characteristics adequately,[9] bending tests of the coated materials were conducted.

Toshihiko Hoshide and **Maki Akamatsu,** Department of Energy Conversion Science, Kyoto University, Sakyo-ku, Kyoto 606-8501, Japan. Contact e-mail: hoshide@energy.kyoto-u.ac.jp.

2. Experimental Procedures

2.1 Material Processing

A commercial borosilicate glass was used as the substrate material. Aluminum of 99.996% purity was adopted as the RF magnetron target material. The glass substrate was a disk with a diameter of 100 mm and a thickness of 2 mm. In this work, aluminum-coated glass was prepared by fixing its film thickness (t_f) at 0.2 μm, although coated materials with other t_f values have been examined in a previous investigation.[10,11]

RF magnetron sputtering was used to coat the borosilicate glass substrates with Al films. The distance between the substrate and target materials was 40 mm. Metallic supporting plates, or bonding plates, onto which the substrate and target materials were fixed, were water cooled during the film-deposition process. Presputtering was carried out for 300 s so that a contaminated layer of target material could be removed. The initial vacuum pressure in a processing chamber was kept at less than 1.3×10^{-4} Pa. The flow rate of argon gas activating the sputtering process in the chamber was maintained at 167 mm^3/s, with the gas pressure in the chamber set at 1.3 Pa. In the sputtering of the Al target material, the initial temperature of the substrate (T_{si}) was set as 293, 473, and 673 K for two levels of RF output power, P_{RF} (i.e., 400 and 800 W).

2.2 Measurements of Film Surface Characteristics

Images of surface areas in each coating film were made through a laser-scanning microscope. They were processed into digital data using a personal computer on which software for image processing was installed. Data on individual areas of a coating film were used to evaluate the roughness and porosity (p), with the roughness and p finally presented as averaged values for the coating film. By using the images processed by the software, the surface roughness (R_a) was evaluated as the centerline average.

In evaluating the p of a film, it was defined as the fraction of the total pore area in a measured surface region. Pores in the measured surface region were identified by an automatic threshold operation in the image-processing software.

2.3 Hardness Test

To avoid the influence of the substrate hardness on the film hardness, the penetrating depth of the indenter was kept between one fifth and one tenth of the t_f.[12] For this situation, a dynamic microhardness tester with an applicable range of indentation forces from 98 μN to 1.96 N was used to measure the film hardness. Using a dynamic microhardness tester, ceramic-coated materials satisfied the aforementioned condition adequately.[10,11] Even though such a microhardness tester was used, the sputtered Al film was so soft that the effect of the substrate hardness could not be avoided. Consequently, Al film hardness was measured using a conventional microhardness tester of the Vickers type. In this case, the measured hardness was considered to be the bulk hardness of the coated material including the substrate hardness. In this experiment, 98 mN was adopted as the peak indentation force, and the indentation time was kept at 15 s.

2.4 Bending Test

For bending tests, plate-type specimens with dimensions of 10 mm in width and 40 mm in length were cut from the coated glass substrates. The bending tests of the coated and non-coated borosilicate glass were conducted using a three-point bend configuration with a span length of 20 mm. The loading rate was controlled so that the rate of nominal stress at the position subjected to the maximum tensile stress in a specimen was 100 MPa/s. In setting a coated specimen on the bend support structure, the coated surface of the specimen was positioned to be in tension. Fifteen specimens were prepared for each sputtering condition. All tests were carried out in ambient conditions (i.e., at 289 ± 2 K and at a relative humidity of 70 ± 8%). The bend strength of the coated and noncoated specimens was calculated as the maximum nominal stress at final failure, irrespective of their actual breaking position.

3. Experimental Results and Discussions

3.1 Characteristics of Coating Film

Higher RF output power results in a higher rate of film formation, as shown in Table 1. The T_{si}, however, does not affect the formation rate significantly. Aluminum films sputtered under almost all conditions were silver in color, like the color of Al itself.

The centerline average roughness (R_a) measured on specimen surfaces coated with Al is shown in Fig. 1, where the R_a is plotted with respect to the T_{si}. It was found that R_a increases with increasing T_{si}. On the other hand, no significant difference due to RF output power was seen, even though the surface of the Al film that was sputtered at a P_{RF} equal to 800 W was a little bit rougher than that sputtered at 400 W. Since the R_a of the substrate glass was 13×10^{-3} μm, the surface coating of the Al film for all sputtering conditions, except when T_{si} was equal to 673 K, was found to be smoother than that of the borosilicate glass surface.

Figure 2 shows the relationship between the p and the T_{si}. As seen in Fig. 2, the p increased as T_{si} increased. In this case, the p increases for the higher value of P_{RF}, even though the p difference due to P_{RF} variation is small.

From the above results, it was found that a smoother and denser film could be formed by decreasing the substrate temperature. This leads to a correlation between roughness and p. In Fig. 3, the R_a was correlated with the p for all sputtering conditions investigated in this work, and the film surface tends to be rougher for coating films with high p.

Table 1 Formation rate of Al film coated on glass

Variables	Radio frequency output power (P_{RF}) 400 W			800 W		
Initial substrate temperature (T_{si}), K	293	473	673	293	473	673
Formation rate, nm/s	1.4	1.6	1.5	3.2	2.4	3.4

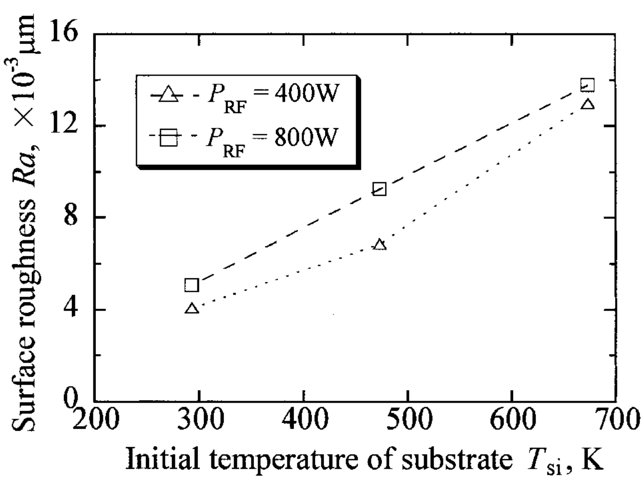

Fig. 1 Variation of R_a with respect to the T_{si}

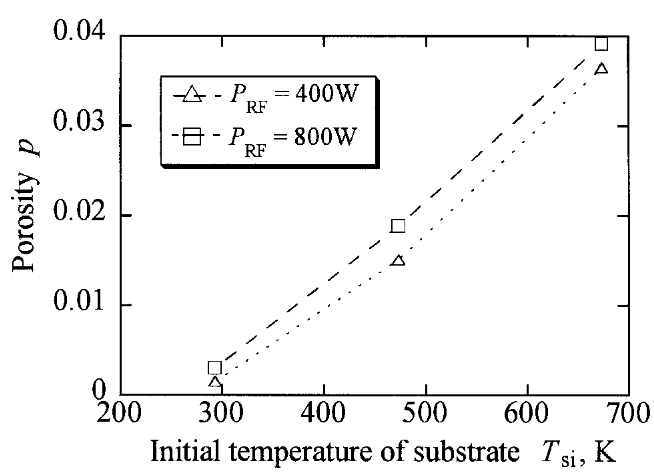

Fig. 2 Variation of p with respect to the T_{si}

3.2 Vickers Hardness

The relationship between Vickers hardness (*HV*) and the initial substrate temperature is shown in Fig. 4. As T_{si} increased, the coated material as well as the substrate glass softened. This trend was mainly caused by the softening of the glass treated at higher temperature. It should be noted that the glass is harder than the Al, and the hardness of the coated material includes both Al and glass. Therefore, as seen in Fig. 4, the hardness of the coated material is lower compared with that of the substrate glass.

In the following discussion, the mean Vickers hardness (HV_m) and the coefficient of variation are dealt with as typical statistical parameters. As is well known, the coefficient of variation, or the ratio of the standard deviation to the mean value, implies the extent of scatter. That is, the scatter of a related random variable is larger for a larger coefficient of variation. Table 2 presents the HV_m values and the coefficient of variation of Vickers hardness (COV_{HV}) with respect to the sputtering condition. As seen in Table 2, COV_{HV} is higher for large values of P_{RF} and tends to decrease for high values of T_{si}. It should be noted that the hardness decreases in the porerich area of a sample but increases in the pore-free regions. This implies that the hardness may change broadly in porous materials, with a wide variation of hardness resulting in a larger COV_{HV}. Therefore, the aforementioned dependence of COV_{HV} on the sputtering condition may be associated with the *p* variation, because the *p* is also found to increase for higher values of P_{RF} and T_{si}, as shown in Fig. 2. Since the average COV_{HV} for the substrate glass is about 0.3 (Table 3), the COV_{HV} for the coated material is smaller than that of the substrate glass.

3.3 Bending Strength

Figure 5 presents the variation of the mean bending strength σ_{fm} with respect to the T_{si}. Table 4 summarizes statistics on the bending strength of Al-coated borosilicate glass, while the statistical properties of the glass strength are listed in Table 3. In these tables, COV_σ is the coefficient of variation of bending strength.

The following discussion summarizes the results from Fig. 5 and Table 4. Generally, substrate glass strength degrades for higher T_{si}, while the strength of the coated material decreases with increasing T_{si}. For the same T_{si}, the strength of the coated material produced under higher P_{RF} conditions is a little bit greater than that produced under lower P_{RF}. As seen in Table 4, the COV_σ for the Al-coated materials did not change systematically on the sputtering conditions. Compared with the COV_σ for the substrate strength (Table 3), the scatter in the strength for the Al-coated material was comparable to that of the substrate glass.

Figure 6 shows examples of the strength data plotted on Weibull probability coordinates, which are obtained for T_{si} values equal to 293 K. The solid and broken lines represent lines drawn by fitting the strength data to the two-parameter Weibull distribution function $F(\sigma_f)$:

Table 2 Vickers hardness of Al-coated glass

	Radiofrequency output power (P_{RF})					
Variables	**400 W**			**800 W**		
T_{si}, K	293	473	673	293	473	673
HV_m	491	423	376	489	433	415
COV_{HV}	0.22	0.14	0.13	0.48	0.16	0.09

T_{si}, initial temperature of substrate; HV_m, mean Vickers hardness; COV_{HV}, coefficient of variation (hardness)

Table 3 Vickers hardness and bend strength of substrate glass

	Temperature of substrate (T_{sg})		
	293 K	**473 K**	**673 K**
HV_m	866	793	704
COV_{HV}	0.23	0.39	0.29
σ_{fm}, MPa	85.0	82.1	65.7
COV_σ	0.14	0.22	0.22

HV_m, mean Vickers hardness; COV_{HV}, coefficient of variation (hardness); σ_{fm}, mean bending strength; COV_σ, coefficient of variation (strength)

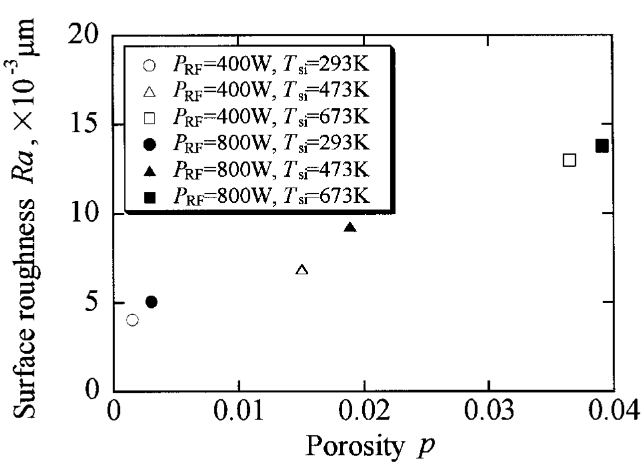

Fig. 3 Relationship between R_a and *p*

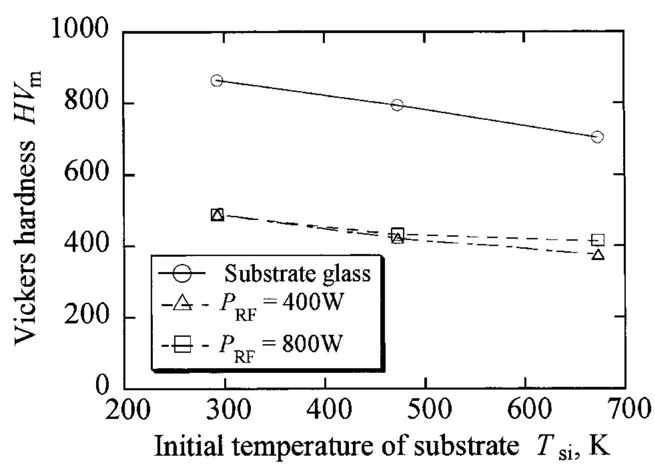

Fig. 4 Variation of hardness with respect to the T_{si}

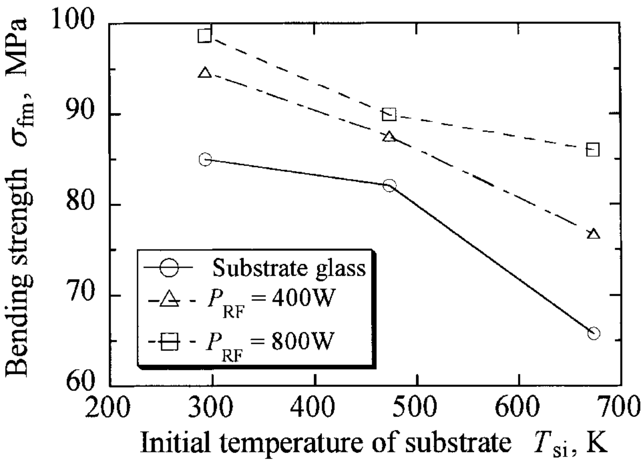

Fig. 5 Variation of σ_{fm} with respect to the T_{si}

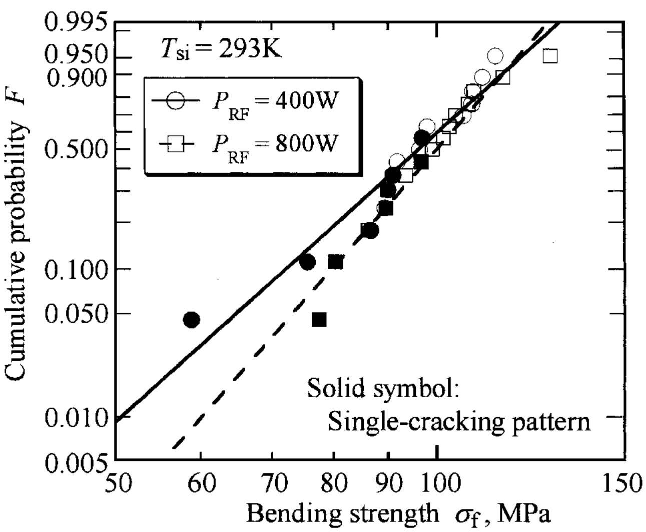

Fig. 6 Weibull distribution of bending strength

$$F(\sigma_f) = 1 - \exp\left\{-\left(\frac{\sigma_f}{\beta}\right)^{\alpha}\right\} \quad \text{(Eq 1)}$$

where α and β are, respectively, the shape and scale parameters. The values for the parameters α and β are listed in Table 4. The shape parameter α is also associated with the scatter range of the strength (i.e., a larger value of α corresponds to less scatter). Similarly to the COV_σ variation, no systematic trend in α-variation is seen with respect to the sputtering condition.

Fracture morphologies of broken specimens were examined, and the cracking pattern was classified into the following two groups. In the first group, specimens broke into two pieces, which resulted from a single crack without branching. In the second group, specimens broke into three or more pieces with crack branching observed. The solid symbols in Fig. 6 indicate those specimens classified into the first group. As seen in Fig. 6, the solid symbols are located in the lower-strength region, and such a trend is confirmed irrespective of the P_{RF} and the T_{si} of the substrate.

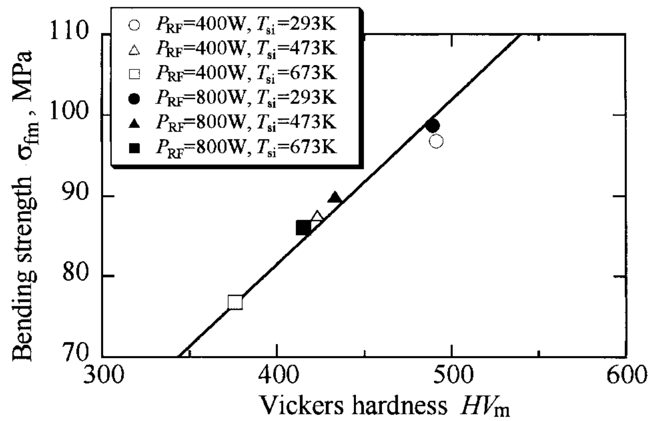

Fig. 7 Relationship between bending strength and hardness

Table 4 Bend strength of Al-coated glass radiofrequency of output power

	P_{RF}					
Variables	**400 W**			**800 W**		
T_{si}, K	293	473	673	293	473	673
σ_{fm}, MPa	96.8	87.5	76.8	98.7	89.9	86.0
COV_σ	0.15	0.21	0.21	0.13	0.11	0.25
Shape parameter α	6.62	4.97	5.14	8.36	9.01	3.77
Scale parameter β, MPa	101.0	95.4	83.4	104.0	101.0	95.6

T_{si}, initial temperature of substrate; σ_{fm}, mean bend strength; COV_σ, coefficient of variation (strength)

3.4 Relationship Between Strength and Hardness

It was observed that the hardness and strength of the substrate glass decreased when the substrate temperature was increased. As mentioned previously, the hardness of coated materials reflects not only the hardness of the Al coating film, but also that of the substrate glass. Therefore, a relation is expected to exist between the hardness and strength of a coated material. In Fig. 7, the bending strength is correlated with the hardness for coated materials. Figure 7 also shows good correspondence between the two, which is represented by the relationship:

$$\sigma_{fm} = 0.204\, HV_m \quad \text{(Eq 2)}$$

Consequently, it is suggested that the strength degradation of the coated material, due to heat treatment, is primarily attributed to glass softening, which is a phenomenon that is sometimes observed at higher temperatures.

4. Conclusion

A commercial borosilicate glass was coated with aluminum of 99.996% purity by RF magnetron sputtering using several conditions. Under the sputtering conditions examined in the present work, dense films were formed on the glass substrate.

The R_a of Al film on the borosilicate glass substrate was less than that of just the substrate glass.

The hardness and three-point bending test results of the coated specimens and the substrate glass were determined, and the effects of the sputtering condition on these properties were investigated. The strength of the coated glass improved relative to that of the uncoated substrate glass, while the hardness of the coated materials was lower than that of the substrate glass. The hardness and strength of the coated materials were lowered by heating the substrate to a higher temperature. However, no remarkable effect of P_{RF} on hardness and strength was identified. Strength degradation was observed for the situation when specimens broke into two pieces. Since the P_{RF} did not affect the hardness and strength, a higher P_{RF} is recommended to form the films more quickly. For improvement of the hardness and strength properties, it is suggested that the temperature of the substrate be kept as low as possible during the sputtering process.

Acknowledgment

This work was supported by Grant-in-Aids for Scientific Research (C)(2) (No. 15560070) from the Japan Society for the Promotion of Science.

References

1. K.H. Kim, K.C. Park, and D.Y. Ma, Structural, Electrical and Optical Properties of Aluminum Doped Zinc Oxide Films Prepared by Radio Frequency Magnetron Sputtering, *J. Appl. Phys.,* Vol 81 (No. 2), 1997, p 7764-7772
2. Y. Fukuma, H. Asada, N. Nishimura, and T. Koyanagi, Ferromagnetic Properties of IV-VI Diluted Magnetic Semiconductor $Ge_{1-x}Mn_xTe$ Films Prepared by Radio Frequency Sputtering, *J. Appl. Phys.,* Vol 93 (No. 7), 2003, p 4034-4039
3. Y. Peng, C. Park, and D.E. Laughlin, Fe_3O_4 Thin Films Sputter Deposited from Iron Oxide Targets, *J. Appl. Phys.,* Vol 93 (No. 10), 2003, p 7957-7959
4. D.-A. Chang, P. Lin, and T.-Y. Tseng, Optical Properties of $ZrTiO_4$ Films Grown by Radio-Frequency Magnetron Sputtering, *J. Appl. Phys.,* Vol 77 (No. 9), 1995, p 4445-4451
5. G.T. Kiehne, G.K.L. Wong, and J.B. Ketterson, Optical Second-Harmonic Generation in Sputter-Deposited AlN Films, *J. Appl. Phys.,* Vol 84 (No. 11), 1998, p 5922-5927
6. H. Mizoguchi, N. Kitamura, K. Fukumi, T. Mihara, J. Nishii, M. Nakamura, N. Kikuchi, H. Hosono, and H. Kawazoe, Optical Properties of $SrMoO_3$ Thin Film, *J. Appl. Phys.,* Vol 87 (No. 9), 2000, p 4617-4619
7. S. Venkataraj, O. Kapperiz, H. Weis, R. Drese, R. Jayavel, and M. Wuttig, Structural and Optical Properties of Thin Zirconium Oxide Films Prepared by Reactive Direct Current Magnetron Sputtering, *J. Appl. Phys.,* Vol 92 (No. 7), 2002, p 3599-3607
8. T.W. Scharf, R.D. Ott, D. Yang, and J.A. Barnard, Structural and Tribological Characterization of Protective Amorphous Diamond-Like Carbon and Amorphous CN_x Overcoats for Next Generation Hard Disks, *J. Appl. Phys.,* Vol 85 (No. 6), 1999, p 3142-3154
9. T. Hoshide, Strength Characteristics of Structural Ceramics, *Mater. Sci. Res. Int.,* Vol 2 (No. 4), 1996, p 220-228
10. T. Hoshide, K. Hayashi, T. Saito, K. Katsuki, and T. Inoue, Mechanical Properties of Borosilicate Glass Coated With Alumina by Sputtering Process, *Mater. Sci. Res. Int.,* Vol 2 (No. 1), 1996, p 33-38
11. T. Hoshide, A. Nebu, and K. Hayashi, Bending Strength of Borosilicate Glass Coated With Alumina and Silicon Carbide by RF Magnetron Sputtering, *JSME Int. J. Ser. A,* Vol 41 (No. 1), 1998, p 332-337
12. P.J. Burnett and D.S. Rickerby, Assessment of Coating Hardness, *Surf. Eng.,* Vol 3 (No. 1), 1987, p 69-76